Manganese removal from aqueous solution using a thermally decomposed leaf

Zhenze Li [a,*], Shigeyoshi Imaizumi [b], Takeshi Katsumi [a], Toru Inui [a], Xiaowu Tang [c], Qiang Tang [c]

[a] GSGES, Kyoto University, Sakyo, Kyoto 606-8501, Japan
[b] Department of Advanced Interdisciplinary Science, Utsunomiya University, 7-1-2, Yoto, Utsunomiya 321-8585, Japan
[c] MOE Key Laboratory of Soft Soils and Geoenvironmental Engineering, Zhejiang University, Hangzhou 310058, China

ARTICLE INFO

ABSTRACT

As a significant agricultural and industrial raw material, Mn(II) has been intensively used and widely distributed in the environment. Recent studies indicate that Mn(II) could cause acute toxicity to aqueous livings and human beings. The treatment of Mn(II) contained wastewater is stringent for environmental preservations. This paper attempts to testify the performance of Mn(II) adsorption by a novel adsorbent, natural leaf that was partially decomposed at moderate temperature. The isothermal adsorption shows high prevalence for Mn(II) with adsorption capacity determined at 61–66 mg g^{-1}. Various factors including adsorbent dosage, pH, temperature and equilibration time were investigated regarding the effects on Mn(II) adsorption. It was shown that a rapid equilibration within 30 min could be achieved at pH values as low as 4.0 while an endothermic and spontaneous process could be disclosed with enthalpy change ranged from 13 to 0.78 kJ mol^{-1} and the entropy change ranged from -35.79 to -11.58 kJ mol^{-1} from 5 to 55 °C, separately. Spectroscopy study revealed chemisorptions relevant to phosphate, ferrous oxide and carbonate groups, and a physisorption on carbon black, which were main components of the adsorbent. No obvious linkage was observed between Mn(II) adsorption and the amine group which is critical to heavy metal adsorption in previous studies. The proposed preparation method and the basic guidelines regarding the adsorbents' selection seem promising in the engineering practices.

© 2009 Elsevier B.V. All rights reserved.

1. Introduction

Manganese is a significant fertilizer for plants, food additive for stocks, catalyst for organic synthesis, basic component for mining, smelting and battery manufacturing. At low levels, usually present as Mn^{2+} in the soil solution, Mn is a nutrient essential to all crops, but it is a toxicant when in excess range of 0.1–0.5 mg/L [1,2]. The abundance of electrons (e−) in acidic soils oriented from decomposed plant residues can make Mn in soil more soluble and potentially more toxic to crops [2]. The mean value of available content of Mn was found to be as high as 850 mg kg^{-1} in soils distributed in central India [3].

The wide industrial utilization makes Mn ubiquitous in many rivers and sediments all over the world. An environmental survey of several rivers of the southern Huasteca area of Mexico revealed high concentrations of manganese (Mn) in the sediments and pore waters [4]. The Huayuan River in Hunan Province in China was reported to be heavily polluted by Mn mining and smelting with the average Mn concentration in the fresh water and sediment at

1.05 mg L^{-1} and 3.84 mg g^{-1}, respectively, about 10 times higher than the legislated concentration permit [5].

As a reducing chemical, Mn(II) could be oxidized to Mn(III) and Mn(IV) by oxygen in contact with air. This will give rise to the chemical oxygen demand (COD) of the wastewater and thus decrease the quality of the water for aquatic livings. Rosko and Rachlin reported the effect of several metals on the growth of a marine diatom and found that the Mn is the least toxicant (25.7 ppm equals to 50% growth depression) compared to Cu (0.033 ppm), Zn (0.27 ppm) and Co (10.2 ppm) [6]. However, acute toxicity of Mn for aquatic microbes was observed and, coexposure to Mn and DDT was significantly more toxic than any of the singly tested compounds [4]. Mn(II) can also cause neurotoxicity to human beings in terms of a syndrome resembling Parkinson's disease as indicated by Roth et al. [7].

As an unstable chemical, the manganese redox cycling in the sediment–water interface region is susceptible to the environmental perturbation. Since the Mn(II) was mobile and abundant in anaerobic conditions, migration of Mn(II) was observed oriented from the bottom towards the upper layer of the sediment in rivers under concentration gradient [8]. After investigation into the Kalix River estuary, Widerlund and Ingri reported that the production rate of dissolved Mn was found exceeded the depositional flux

---

of nondetrital Mn by a factor of about 6 [9]. Upwardly diffusing pore-water Mn is effectively oxidized and trapped in the oxic surface layer of the sediment, resulting in negligible benthic effluxes of Mn. Thus an accumulation of Mn in the interface will be formed naturally and gradually.

Genc et al. attempted to remove manganese from naturally polluted river sediment (alkaline, had 20% illite clay) by applying an electrokinetic remediation technique [10]. The laboratory scale test showed that the removal efficiency of manganese was as low as 18%. Once polluted, the soil will be very hard to be remediated. The treatment of wastewater in the point source of such pollution becomes critical to avoid such shortcomings.

Adsorption has been widely used in wastewater treatment for decoloring and COD decreasing purpose. Adsorbents for heavy metals have been intensively investigated recently [11–16]. Efforts are devoted to decrease the cost of the adsorbent as well as to improve the adsorption affinity and adsorption capacity. The authors have reported a method to turn the natural leaf into an effective adsorbent for Pb(II), Zn(II), etc. However, the adsorption behavior of this sorbent towards Mn(II) remains unclear. Since Mn(II) is a reductive reagent and prone to be changed in chemical state, the relevant adsorption mechanism on the prepared adsorbent might be different from that of the stable heavy metals. Amine was reported abundant in leaf acting as a major sorption site for heavy metals [15]. However, few researches are available as to the possibility of Mn(II) adsorption on this functional group. Accordingly, this paper is intended to (1) investigate the performance of a thermally decomposed leaf (TDL) in adsorption of Mn(II) from water; (2) evaluate the effect of various environmental factors; (3) unravel the mechanism of Mn(II) adsorption on the sorbent.

2. Materials and methods

2.1. Sorbent preparation

Fallen *Firmiana simplex* L. was sampled in autumn, oven dried aerobically at 45 °C overnight, pulverized to pass mesh screen ($d < 355 \pm 13\,\mu m$) and then stored in plastic bags [15]. The leaf powder was calcined in a sealed oven at 250 °C for 5 h with anaerobic condition. There was no gas supply during the calcination process. The obtained decomposed leaf was collected and stored for further test.

Stock solution of Mn(II) ($2.0\,g\,L^{-1}$) was prepared by dissolving 5.765 g $MnSO_4$ into 1000 mL de-ionized water. Conical flasks and centrifuge tubes were immersed in 0.01 M HNO_3 solution overnight to get cleaned and then rinsed three times with de-ionized water.

The Mn(II) laden sorbent was obtained from the centrifuged sediment of the sorbent at 1400 A-g for 5 min after equilibrium adsorption test (dosage $10\,g\,L^{-1}$, $600\,mg\,L^{-1}$ Mn(II), 24 h, 55 °C).

2.2. Characterization of the sorbent

The FT-IR spectra of the sorbents (natural sorbent and Mn(II) laden sorbent) were conducted by Nexus-670 (Nicolet, USA) to specify the contained functional groups. The samples weighed 1.0 g were dried under infrared radiation for 10 min, mixed with KBr (analytical grade), ground into fine powder, compressed into a translucent slice supported by a punched paper under 40 MPa and finally exposed to infrared radiation to determine the IR absorption spectroscopy. The XRD spectra of the both sorbents were obtained by D/MAX-RA apparatus (Rigaku Corporation, Japan) with the assistance of engineers in the university.

2.3. Experiments

2.3.1. Effect of adsorbent dosage

The adsorbent dosage in the aqueous solution was increased from 0.5 to 1, 2, 5, 10 and $20\,g\,L^{-1}$ in this test. The initial Mn(II) concentration (50, 100 and $200\,mg\,L^{-1}$) was prepared by diluting the stock solution into flasks which were then transferred to a thermostatic agitator (25 °C), and equilibrated for 24 h. The mixture was poured to a centrifuge tube and then subject to centrifuge at 1400 A-g for 5 min. The supernatant was sampled to determine the equilibrium Mn(II) concentration by Atomic Absorption Spectroscopy (AAS, AAS Meter, General Analysis, China). Blank tests and duplicates were both conducted.

2.3.2. Effect of pH

The adsorbent dosage was adjusted to $10\,g\,L^{-1}$ with initial Mn(II) concentration at $100\,mg\,L^{-1}$. The pH of the mixture was regulated by 0.01–0.1 M HNO_3 or NaOH solution until the pH_i was close to the target value ranged from 2.0 ± 0.2 to 10.0 ± 0.2 with an overall increment of 1.0. The flasks were then agitated at 25 °C for 24 h. The equilibrium pH of the mixture was measured using a glass potentialmeter once the test was stopped. The mixture was then centrifuged at 1400 A-g for 5 min in order to obtain the supernatant of which the Mn(II) concentration was determined by AAS.

2.3.3. Adsorption kinetics

The adsorbent dosage was prepared to be $10\,g\,L^{-1}$ for three sets of sample mixtures with initial Mn(II) concentrations varied from 50, 100 to $200\,mg\,L^{-1}$. The equilibration temperature was maintained constant at 25 °C. In order to measure the solute concentration at specific times, the test durations were increased from 3 to 6, 9, 12, 15, 20, 40, 60, 120, 180, 240 and 300 min. At the end of each test, the mixture was taken out of the agitator and centrifuged at 1400 A-g for 3 min. The Mn(II) concentration in the supernatant was determined by AAS. Blank tests and duplicates were both conducted.

2.3.4. Adsorption isotherms at different temperatures and thermodynamics

The sorbent ($10\,g\,L^{-1}$) was blended with 11 sets of Mn(II) solution with varied initial concentrations from 25 to $1200\,mg\,L^{-1}$ (25, 50, 100, 200, 300, 400, 500, 600, 800, 1000 and $1200\,mg\,L^{-1}$). The equilibration temperature was maintained constant for each set of isothermal test. Different series of isotherm were determined at increased temperature from 5 to 55 °C with an increment of 10 °C. All samples were equilibrated for 24 h in an agitator and the equilibrium Mn(II) concentrations were measured by AAS. Control and parallel tests were conducted.

3. Results and discussion

3.1. Characterization of the sorbent

Fig. 1 shows the IR spectrum of the prepared adsorbent (a). Characteristic bands could be identified and correlated to OH, N–H, C=O, P=O, Fe–O groups, etc. Hydroxyl group (OH) was found at wavenumber 3440 cm^{-1} with a broad and strong adsorption pattern. The bands at 1620, 1450, 1320 cm^{-1} could be assigned to amine group (N–H). The fingerprint bands at 1120, 876 and 715 cm^{-1} could be related to C=O groups. The bands at 478 and 595 cm^{-1} could be linked to the P=O group of phosphate and the Fe–O group, respectively [15].

Fig. 2 shows the XRD spectra of the adsorbent TDL (a) and relevant mineral constituents. The most intensive band at $2\theta = 26.63°$ can be assigned to carbon black which is possibly the most
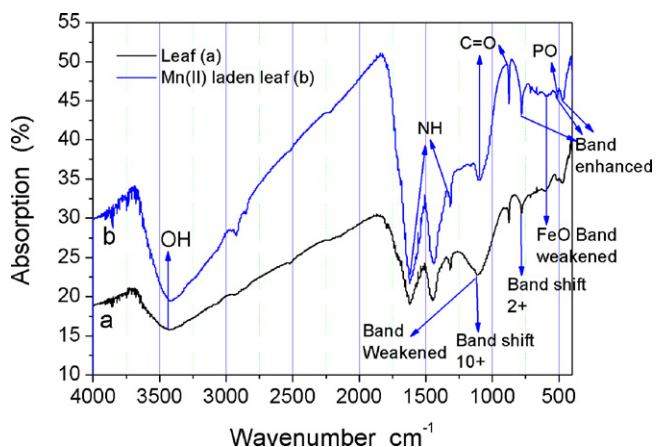
Fig. 1. FT-IR spectra of the TDL (a) and Mn(II) laden TDL (b).

abundant composition in the sorbent. Sodium hydrate phosphate, whewellite, calcite, albite, calcium phosphate, etc. were also observed in the sorbent. These mineral components confirmed the information obtained from the IR spectrum. Phosphate and carbonate are linked to P=O and C=O groups, respectively. Since amine is always contained in organic molecules, the relevant feature is difficult to be observed in XRD spectrum. The absence of this group in XRD spectrum does not mean the presence of this functional group in the sorbent is questionable. Nitrogen is a significant nutritional composition for plants and leaves were reported with high percentage of N mass ratio (20–35 $mg\,g^{-1}$) [17]. Carbon black was reported capable of strongly adsorbing organic molecules [18]. In the following sections, the role of carbon black in Mn(II) adsorption will be discussed.

3.2. Effect of adsorbent dosage

Fig. 3 shows the effect of adsorbent dosage on unit Mn(II) adsorption amount. A sudden reduction in adsorption amount from 99.5 to 10.0 $mg\,g^{-1}$ could be observed with increasing TDL dosage from 0.5 to 5.0 $g\,L^{-1}$. The curve flattened off with further increase in the adsorbent dosage. Within the dosage range from 2.5 to 20 $g\,L^{-1}$, the unit adsorption amount was found increased with increasing initial Mn(II) concentration, while the opposite phenomenon was found at dosage 1.0 $g\,L^{-1}$. At 0.5 $g\,L^{-1}$ dosage, the highest adsorption amount of each set of test was determined at 99.5, 48.8 and
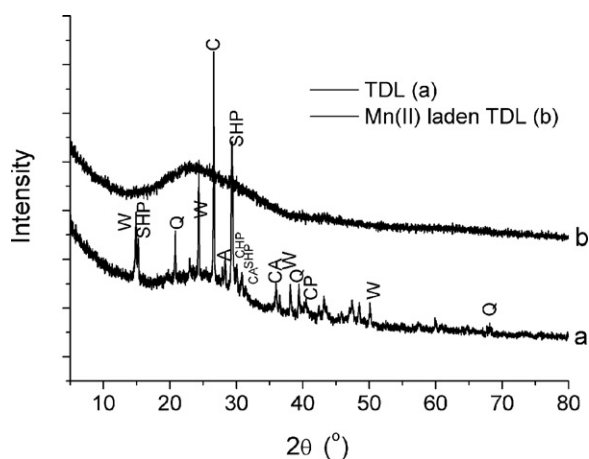

Fig. 2. XRD spectra of the TDL (a) and Mn(II) laden TDL (b) (A: albite; C: carbon; CA: calcite; CHP: calcium hydroxide phosphate; CP: calcium phosphate; Q: quartz; SHP: sodium hydrogen phosphate hydrate; W: whewellite).
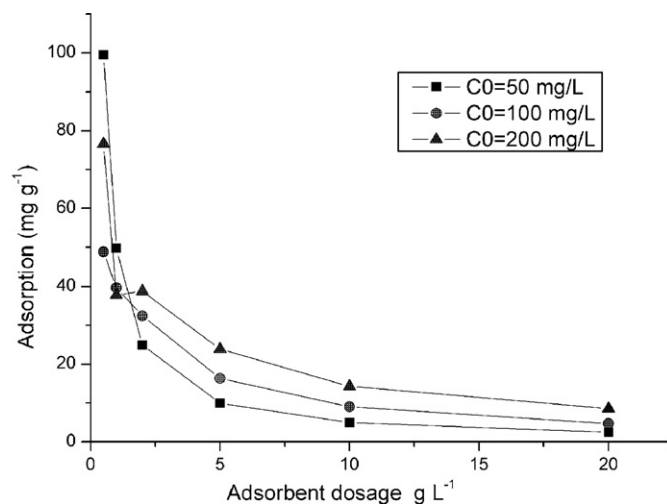

Fig. 3. Effect of adsorbent dosage on unit Mn(II) adsorption amount.

76.6 $mg\,g^{-1}$ for solutions with initial concentration at 50, 100 and 200 $mg\,L^{-1}$, separately.

The unit Mn(II) adsorption amount on the sorbent decreased with increasing initial Mn(II) concentration when the dosage was less than 2.0 $g\,L^{-1}$. This feature might be caused by the pH reduction resulted from the increase in Mn(II) concentration. Since both the initial solute concentration and the equilibrium pH could affect the adsorption amount, the balance between these two parts would lead to a complex performance in the adsorption equilibrium. A dosage at 0.5 $g\,L^{-1}$ will not have enough capacity to buffer the pH change in the solution, thus the pH reduction caused by increased Mn(II) concentration might be predominant which will decrease the unit adsorption amount.

3.3. Effect of pH

Fig. 4 shows the effect of pH on Mn(II) removal percentage. The increase in pH_i from 1.8 to 3.84 gives a sudden rise to the removal percent of Mn(II) from 0 to 99.0% from the solution. Further increase in pH did not affect the $R\%$ obviously. The pH_e was found to be close to the pH_i at $pH_i < 3.84$, larger than the pH_i in the range from 3.84 to 7.30, but turned to be less than the pH_i, flattened and finally reached 8.0 at $pH_i > 7.30$. The TDL demonstrates a bit alkalinity which could
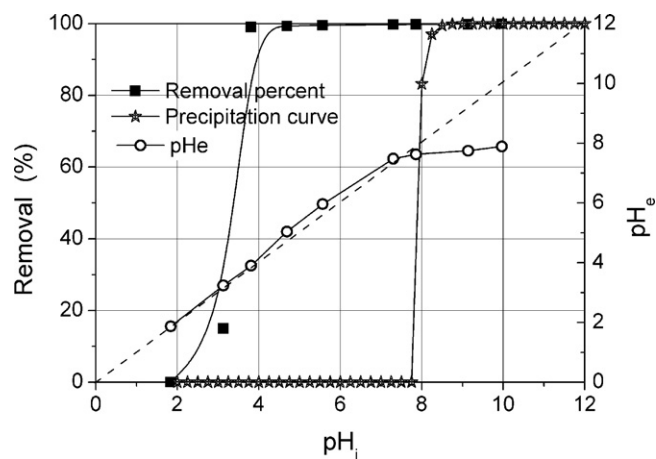

Fig. 4. Effect of pH on Mn(II) removal percentage and Mn(II) precipitation curve ($C_0 = 100\,mg\,L^{-1}$, dosage 10 $g\,L^{-1}$, $T = 25\,°C$; precipitation curve was calculated by Visual MINTEQ v 2.3 with initial conditions as: 100 $mg\,L^{-1}$ $MnSO_4$, 25 °C, pE = 5.0 [19]).
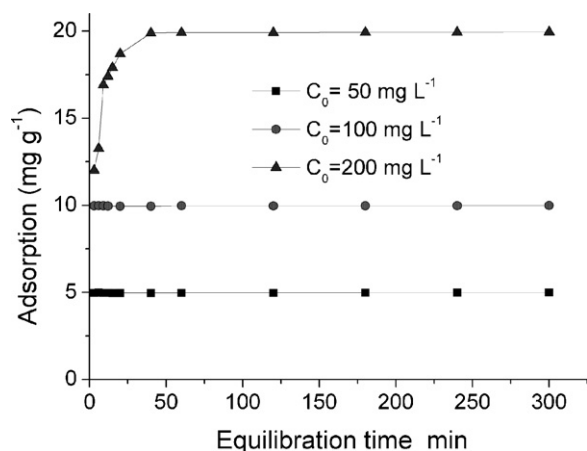
Fig. 5. Variation of unit Mn(II) adsorption amount with equilibrium duration.

be ascribed to the amine and carbonate groups in the sorbent as confirmed by the IR spectrum. Amine group exhibits amphoteric properties and could act as a buffer within a certain pH ranges, in agreement with the observation in Fig. 4.

The precipitation curve for Mn(II) was calculated by a thermo-dynamically based software Visual MINTEQ v 2.3. The soil redox potential (pE) was reported in the range from −3.1 to 7.0 (−182 to +413 mV) [19]. Accordingly, the pE was fixed at the middle point 5.0 in this study in order to calculate the precipitation behavior of Mn(II) in the aqueous solution.

The precipitation of Mn(II) was found started at pH 7.75 and reached maximum at pH 8.75. The huge gap between the adsorption curve and the precipitation curve indicates a strong adsorption affinity from the sorbent towards Mn(II). At pH values as low as 4.0, the TDL could nearly completely remove the dissolved Mn(II) from solution, making it a very promising adsorbent in wastewater treatment. On the other hand, the Mn(II) laden adsorbent could also be refreshed for recycling usage by acidic solution at pH < 2.0.

3.4. Adsorption kinetics

Fig. 5 shows the effect of equilibrium duration on the adsorption amount of Mn(II) on unit TDL. The adsorption equilibrium was rapidly reached within 3 min for solutions at $C_0 = 50$ and 100 mg L^{-1}. An increase in initial Mn(II) concentration at $C_0 = 200$ mg L^{-1} resulted in an extended equilibrium duration to about 30 min, indicating a gradually decreased adsorption affinity with increasing solute concentration. This might give a hint that the kinetic process involves a rapid adsorption with specific adsorption site and a slow adsorption with weak bonding site or in terms of mass migration inwards the micropores in the sorbent.

The test data were analyzed using three kinetic models as follows. The pseudo-first order kinetic equation is written as

$$q = q_e(1 - e^{-k_1 t}) \tag{1}$$

where q_e and q are the amounts of adsorbate per unit weight of adsorbent at equilibrium and any time, respectively (mg g^{-1}), and k_1 the pseudo-first order rate constant (min^{-1}).

The pseudo-second order kinetic equation is in the form of

$$\frac{t}{q} = \frac{1}{k_2 q_e^2} + \frac{t}{q_e} \tag{2}$$

where k_2 (g mg^{-1} min^{-1}) is the relevant rate constant and q_e the predicted adsorption capacity (mg g^{-1}).

The equation on the intraparticle diffusion model with an assumption that the sorption is in terms of pore-filling pattern is

Table 1
Predicted kinetic constants for Mn(II) adsorption on TDL.

	C_0 (mg L^{-1})		
	50	100	200
1st order kinetics			
q_e (mg g^{-1})	4.9793	9.9698	19.524
k_1 (min^{-1})	2.1827	5.31	0.2296
R	1	1	0.9866
2nd order kinetics			
q_e (mg g^{-1})	4.996	9.986	20.088
k_2 (g mg^{-1} min^{-1})	1.4495	1.4533	0.0309
R	1	1	1
Intraparticle diffusion model			
k_{int} (mg g^{-1} min$^{-1/2}$)	0.0013	0.0012	0.3521
R	0.5971	0.4754	0.7003

expressed as

$$q = k_{int} t^{1/2} \tag{3}$$

where k_{int} is the constant of diffusion rate (mg g^{-1} min$^{-1/2}$).

From Table 1 the 1st and 2nd order kinetics were both found fit the test result well based on the correlation coefficient. The predicted adsorption capacities were consistent with the test results. The constants k_1 and k_2 indicating the adsorption rate, were found increased a little when the initial concentration of Mn(II) increased from 50 to 100 mg L^{-1}, and then significantly decreased by more than 96% when C_0 increased to 200 mg L^{-1}. Overall, the adsorbent prepared in this paper could rapidly remove the Mn(II) from solution.

3.5. Adsorption isotherm

Fig. 6 shows the various adsorption isotherms at different temperatures. A typical 'H' type isotherm could be identified. The isotherms at $C_e < 2.5$ mg L^{-1} ($C_0 < 600$ mg L^{-1}) were coincident with each other and appeared not to be affected by the temperature. Obvious difference between isotherms occurred at $C_e > 150$ mg L^{-1}. The adsorption of Mn(II) on TDL could be regarded as a strong bond in terms of chemisorption with high priority. Once the adsorption capacity was reached, the adsorption of Mn(II) might be involved in a physical process and thus prone to be affected by the temperature.

The Langmuir model assumes a homogeneous monolayer surface sorption and can be written as
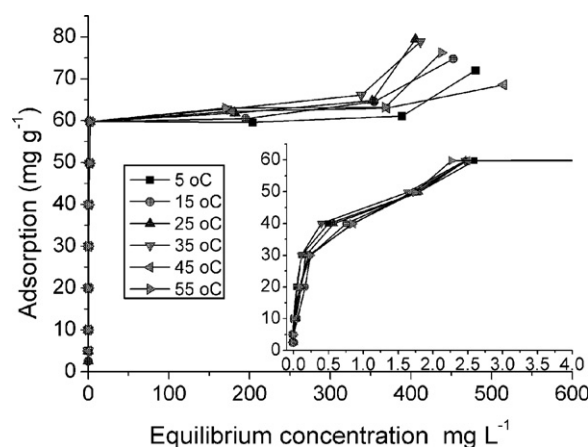
$$\frac{1}{q_e} = \frac{1}{Q} + \frac{1}{bQC_e} \tag{4}$$

Fig. 6. Adsorption isotherm of Mn(II) on TDL at various temperatures.

Table 2
Predicted isothermal constants for Mn(II) adsorption on TDL.

	Temperature (°C)					
	5	15	25	35	45	55
Langmuir model						
Q (mg g^{-1})	61.63	65.96	66.57	65.59	62.95	65.82
b	6.56	2.65	3.46	5.86	3.76	3.04
R	0.975	0.985	0.980	0.975	0.985	0.980
Freundlich model						
K_F (mg g^{-1})	33.40	32.39	33.79	34.88	33.18	33.49
n	8.177	7.442	7.484	7.688	8.033	7.602
R	0.868	0.876	0.894	0.901	0.879	0.891
D-R model						
$\ln q_m$ (mol g^{-1})	−6.032	−5.910	−5.935	−6.350	−6.029	−5.943
k	0.0023	0.0025	0.0021	0.0019	0.0018	0.0018
E	−14.78	−14.29	−15.43	−16.40	−16.76	−16.90
R	0.875	0.906	0.932	0.907	0.893	0.928

where Q is the maximum sorption capacity of the adsorbent (mg g^{-1}), and b (L mg^{-1}) the Langmuir constant.

The Freundlich model assumes a non-ideal adsorption and can be expressed as

$$q_e = K_F C_e^{1/n} \tag{5}$$

where K_F and n are the Freundlich constants related to the adsorption capacity and adsorption intensity of the sorbent, respectively.

The D-R model assumes a uniform pore-filling sorption and can predict the free sorption energy change which reflects the adsorption type. The D-R model is written as

$$\ln q_e = \ln q_m - k\varepsilon^2 \tag{6}$$

where q_m is the maximum sorption capacity (mol g^{-1}), k a model constant related to the free sorption energy and ε the Polanyi potential, which is written as

$$\varepsilon = RT \ln \left(1 + \left(\frac{1}{C_e}\right)\right) \tag{7}$$

The mean free energy of sorption (E) is

$$E = -\frac{1}{\sqrt{2k}} \tag{8}$$

Basically, the adsorption is physical adsorption when $|E|$ is between 1.0 and 8.0 kJ mol^{-1}.

Table 2 shows the predicted isothermal constants. The Langmuir model could best fit the test results due to the high correlation coefficients ($R > 0.975$). The sorption capacity was predicted in the range from 61.63 to 66.57 mg g^{-1}. D-R model, although appeared with less correlation coefficients than Langmuir model, could predict the free adsorption energy which could help to understand the adsorption mechanism. As the free adsorption energy E is ranged from −16.90 to −14.29 kJ mol^{-1}, the adsorption of Mn(II) on the prepared sorbent could be considered as a chemisorptions with high adsorption affinity. This feature is in agreement with the previous conjectures according to the kinetic studies.

3.6. Thermodynamics

According to thermodynamic theory, the following Gibbs free energy equation can be written as

$$\Delta G^0 = -RT \ln K_D \tag{9}$$

$$\Delta G^0 = \Delta H^0 - T \Delta S^0 \tag{10}$$

where ΔH^0 is the enthalpy change, ΔG^0 the Gibbs free energy change, ΔS^0 the entropy change, R the ideal gas constant (8.314 J mol^{-1} K$^{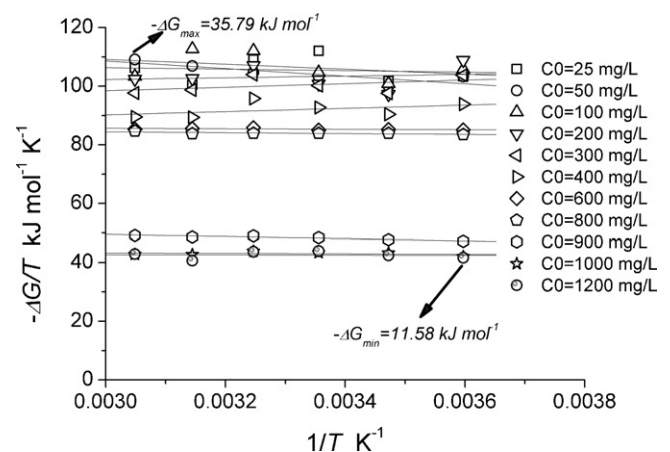-1}$), T the absolute temperature (K) and K_D is the distribution coefficient of the solute between the adsorbent and the solution in equilibrium (q/C_e, mL g^{-1}).

Fig. 7 shows the linearized form of the test results by the thermodynamic equations. The obtained model constants are screened on the basis of correlation coefficient and those with high R ($R > 0.80$) are shown in Table 3. The enthalpy and entropy changes are both positive, indicating an endothermic and spontaneous adsorption, respectively. The increase in initial Mn(II) concentration results in decreased enthalpy and entropy changes, which are separately ranged from 13.00 to 0.78 kJ mol^{-1} and from 147.61 to 45.60 J mol^{-1} K^{-1}. Decreased entropy at higher Mn(II) concentrations suggests reduction in adsorption preference, corresponding to the flattened features in adsorption isotherms.

The predicted change of Gibbs free energy was in the range of −35.79 to −11.58 kJ mol^{-1}. This is consistent with the free adsorption energy predicted by D-R model (−14.29 to −16.90 kJ mol^{-1}). The increase in temperature will somewhat enhance the performance in Mn(II) adsorption. However, this effect was rather limited since the different adsorption isotherms at various temperatures shown in Fig. 6 were close to each other at $C_e < 2.5$ mg L^{-1}

Table 3
Thermodynamic constants of Mn(II) adsorption on TDL.

	C_0 (mg L^{-1})			
	50	100	900	1000
ΔS (J mol^{-1} K^{-1})	147.61	134.42	60.15	45.60
ΔH (kJ mol^{-1})	13.00	8.42	3.55	0.78
R	0.84	0.93	1.00	0.92

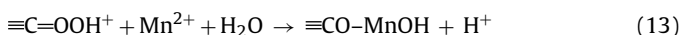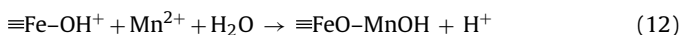**Fig. 7.** Thermodynamically linearized form of Mn(II) adsorption on TDL.

($C_0 < 800\,\text{mg}\,\text{L}^{-1}$). In case of physisorption, the increased temperature could significantly affect the adsorption equilibrium and even be used to recycle the used adsorbent. The negligible impact of temperature might be related to the strong adsorption bond (chemisorption) between the adsorbent and Mn(II), which weakens the effect of temperature on the adsorption equilibrium.

3.7. Mechanism discussion

As discussed in the previous sections, the adsorption of Mn(II) on the partially decomposed leaf is mainly a chemisorptions with little relevance to the temperature impact. Spectra studies by IR and XRD could provide much more specific information on the sorption mechanism.

Fig. 1 shows the IR spectrum of Mn(II) laden TDL (line b). The adsorption of Mn(II) could be ascribed to P=O, Fe–O and C=O groups due to the changes in band intensity and position. After Mn(II) adsorption, the band at $876\,\text{cm}^{-1}$ relative to C=O group was weakened in band strength and shifted to 10+ wavenumber. The band for Fe–O group was found weakened while the band for P=O group was strengthened after Mn(II) adsorption. The bands relevant to OH and NH groups did not show observable changes.

Accordingly, the chemical reaction between functional groups and Mn(II) could be written in the following forms:

$$HPO_4{}^{2-} + Mn^{2+} \rightarrow MnHPO_4\downarrow \tag{11}$$

$$\equiv\text{Fe–OH}^+ + Mn^{2+} + H_2O \rightarrow \equiv\text{FeO–MnOH} + H^+ \tag{12}$$

$$\equiv\text{C=OOH}^+ + Mn^{2+} + H_2O \rightarrow \equiv\text{CO–MnOH} + H^+ \tag{13}$$

Another proof for these listed chemical reactions is the XRD pattern of the Mn(II) laden TDL as shown in Fig. 2, line b. The sharp bands corresponding to inorganic components in TDL were found disappeared after Mn(II) adsorption. This might be resulted from the dissolution/transformation of these mineral constituents after reacted with Mn(II), further verifying the speculation of chemisorptions.

As to amine group, it is a bit strange to be found irrelevant to Mn(II) adsorption. Previous study has confirmed the significant contribution to metal adsorption from amine group [15]. One special feature of the adsorbent prepared by the method proposed in this paper is to preserve the abundant nitrogen component in the natural leaf and transform it into amine group. But it appears to advise us that the metal type and the chemical state (redox potential) should also be taken into account when designing a novel adsorbent.

The XRD spectrum of TDL in Fig. 2 shows that abundant carbon black was formed during the sorbent preparation process. Reference shows that carbon is effective to adsorb heavy metals [20,21]. The micropores contained in carbon might be a potential space for Mn(II) adsorption and the only possible route is in the form of intraparticle diffusion. The kinetic adsorption study enclosed two patterns of Mn(II) adsorption: (1) rapid surface adsorption ($C_0 = 50$ and $100\,\text{mg}\,\text{L}^{-1}$ shown in Fig. 5); (2) comparatively slow diffusion inwards micropores in the sorbent at higher solute concentrations ($C_0 = 200\,\text{mg}\,\text{L}^{-1}$ shown in Fig. 5). The analysis of the test data using kinetic models also confirmed these speculations.

Table 4 shows the reported Mn(II) adsorbent and relevant adsorption capacity. The adsorbent prepared in this study gave the best performance in adsorption capacity. Therefore the proposed preparation method and the basic guidelines regarding the adsorbents' selection seem promising in the engineering practices. The reported Mn(II) adsorption capacity on carbons ($<2.5\,\text{mg}\,\text{g}^{-1}$) appeared significantly less than the TDL reported in this study ($>61\,\text{mg}\,\text{g}^{-1}$). The presence of active chemicals (phosphate, carbonate and ferrous oxide, etc.) played major roles in Mn(II) adsorption

Table 4
Reported Mn(II) adsorbent and relevant adsorption capacity.

Adsorbent	Capacity ($\text{mg}\,\text{g}^{-1}$)	Reference
Alginate gel beads	3.64	[22]
Black carrot residues	5.17	[23]
Carbon nanotube	<2.5	[24]
Fly ash	0.2	[25]
Kaolinite	0.446	[26]
Tannic laden activated carbon	1.13	[27]
Thermally decomposed leaf	>61	This study

from aqueous solutions. However, the effect of carbon on Mn(II) adsorption could not be ignored because it could provide matrix carrier for surface chemical precipitate resulted from reaction between heavy metals and active chemicals contained in the adsorbent [28].

This study dealt with the Mn(II) adsorption performances as well as the related mechanisms. We found that the adsorbent can strongly adsorb Mn(II) in a manner of chemisorption, rather than physisorption via carbon which is very abundant in the adsorbent. The chemisorption is related to several functional groups, which has been well documented, but less observed in one single adsorbent. This is the uniqueness of our study: a special complex with various adsorption sites acting as a systematic organism exerting positive influence on metal uptake. After carefully discussing the effects of chemically active functional groups, we identified the role of amine group in Mn(II) adsorption which was unavailable in literatures. This study specifically revealed the irrelevance between amine and Mn(II) for the first time. And this could be considered as a basic principle in adsorbent selection for metals.

Besides, the adsorbent obtained in this study appeared to have the highest Mn(II) sorption capacity during all the reported data as shown in the last table. The authors believe that this feature could attract wide interests from the common readers of the *Journal of Hazardous Materials*.

We studied the adsorption performance of a waste material and developed a novel method to transform a common natural product into a precious material showing promising potential in engineering practice. We are also contributing to the low-carbon economy in terms of utilizing a natural leaf which is hugely produced worldwide and readily decomposed biologically to obtain a series of rather stable constituents, i.e. carbon which is stable and resistant to microbial digestion. This is not only a novelty in research, but also a contribution to the low-carbon economy which is critical to relieve the green house effect. Cutting down the emission of carbon dioxide might be largely dependent on the public care and support, i.e. the publication of relevant studies like this manuscript. We will then have the hope to pass on the next generation a better and cooler earth.

4. Conclusions

(1) Thermally decomposed leaf could effectively remove Mn(II) from solution with the adsorption capacity determined at $61–66\,\text{mg}\,\text{g}^{-1}$.
(2) The adsorbent dosage and pH show more obvious effect on Mn(II) adsorption than temperature and equilibration time.
(3) The adsorption of Mn(II) on TDL is rapidly equilibrated within 30 min.
(4) Thermodynamic study shows the adsorption as an endothermic and spontaneous process with enthalpy change ranged from 13 to $0.78\,\text{kJ}\,\text{mol}^{-1}$ and the entropy change ranged from -35.79 to $-11.58\,\text{kJ}\,\text{mol}^{-1}$ from 5 to $55\,^\circ\text{C}$.
(5) Mn(II) adsorption on TDL involves chemisorptions relevant to phosphate, ferrous oxide, carbonate and physisorption relevant

to carbon black containing abundant micropores. Amine was found irrelevant to Mn(II) adsorption.

Acknowledgement

References

[1] W.J. Horst, H. Marschner, Effect of silicon on manganese tolerance of bean plants, Plant Soil 50 (1978) 287–303.

[2] College of Tropical Agriculture and Human Resources (CTAHR), Managing Soil Manganese Toxicity, CTAHR, University of Hawaii at Manoa, Hawaii, USA, 1998.

[3] N.K. Jaiswal, K.S. Patel, Manganese soil pollution in Central India, Goldschmidt Conf. Abstr. A422 (2008) (Elsevier B.V., Netherlands).

[4] J. Mejía-Saavedra, et al., Effect of coexposure to DDT and manganese on freshwater invertebrates: pore water from contaminated rivers and laboratory studies, Environ. Toxicol. Chem. 24 (2005) 2037–2044.

[5] N. Hu, et al., Metal pollution in Huayuan River in Hunan Province in China by manganese sulphate waste residue, Bull. Environ. Contam. Toxicol. 83 (2009) 4583–4590.

[6] J.J. Rosko, J.W. Rachlin, The effect of copper, zinc, cobalt and manganese on the growth of the marine diatom *Nitzschia closterium*, Bull. Torrey Bot. Club 102 (1975) 100–106.

[7] J.A. Roth, C. Horbinski, D. Higgins, P. Lein, M.D. Garrick, Mechanisms of manganese-induced rat pheochromocytoma (PC12) cell death and cell differentiation, Neurotoxicology 23 (2002) 147–157.

[8] M. Kataoka, M. Matsuo, Chemical speciation of manganese in the estuarine and tideland sediments, Photon Factory Activity Report 2002 (No. 20) Part B (2003) 21.

[9] A. Widerlund, J. Ingri, Redox cycling of iron and manganese in sediments of the Kalix River estuary, Northern Sweden, Aquatic Geochem. 2 (2) (1996) 185–201.

[10] A. Genc, G. Chase, A. Foos, Electrokinetic removal of manganese from river sediment, Water Air Soil Pollut. 197 (2009) 131–141.

[11] J. Rincón, F. González, A. Ballester, M.L. Blázquez, J.A. Muñoz, Biosorption of heavy metals by chemically-activated alga *Fucus vesiculosus*, J. Chem. Technol. Biotechnol. 80 (2005) 1403–1407.

[12] Y. Zhang, C. Banks, The interaction between Cu, Pb, Zn and Ni in their biosorption onto polyurethane-immobilised *Sphagnum moss*, J. Chem. Technol. Biotechnol. 80 (2005) 1297–1305.

[13] C. Cabrera, C. Gabaldón, P. Marzal, Sorption characteristics of heavy metal ions by a natural zeolite, J. Chem. Technol. Biotechnol. 80 (2005) 477–481.

[14] J. Goel, K. Kadirvelu, C. Rajagopal, V.K. Garg, Investigation of adsorption of lead, mercury and nickel from aqueous solutions onto carbon aerogel, J. Chem. Technol. Biotechnol. 80 (2005) 469–476.

[15] Z. Li, X. Tang, Y. Chen, et al., Activation of *Firmiana simplex* leaf and the enhanced Pb(II) adsorption performance: equilibrium and kinetic studies, J. Hazard. Mater. 169 (2009) 386–394.

[16] G.S. Gupta, A.K. Singh, B.S. Tyagi, G. Prasad, V.N. Singh, Treatment of carpet and metallic effluents by China clay, J. Chem. Technol. Biotechnol. 55 (1992) 277–284.

[17] T.M. DeJong, J.F. Doyle, Seasonal relationships between leaf nitrogen content (photosynthetic capacity) and leaf canopy light exposure in peach (*Prunus persica*), Plant Cell Environ. 8 (1985) 701–706.

[18] A.M. Accardi-Dey, P.M. Gschwend, Reinterpreting literature sorption data considering both absorption into organic carbon and adsorption onto black carbon, Environ. Sci. Technol. 37 (2003) 99–106.

[19] E.T. Smiley, J.J. Kielbaso, P.V. Nguyen, Soil factors associated with manganese deficiency of urban sugar and red maples, J. Arboriculture 12 (1986) 169–173.

[20] J. Rivera-Utrilla, M.A. Ferro-Garcia, A. Mata-Arjona, C. González-Goméz, Studies on the adsorption of caesium, thallium, strontium and cobalt radionuclides on activated carbons from aqueous solutions, J. Chem. Technol. Biotechnol. 34 (1984) 243–250.

[21] X. Peng, J. Jia, Z. Luan, Oxidized carbon nanotubes for simultaneous removal of endrin and Cd(II) from water and their separation from water, J. Chem. Technol. Biotechnol. 84 (2009) 275–278.

[22] T. Gotoh, K. Matsushima, K. Kikuchi, Adsorption of Cu and Mn on covalently cross-linked alginate gel beads, Chemosphere 55 (2004) 57–64.

[23] F. Güzel, H. Yakut, G. Topal, Determination of kinetic and equilibrium parameters of the batch adsorption of Mn(II), Co(II), Ni(II) and Cu(II) from aqueous solution by black carrot (*Daucus carota* L.) residues, J. Hazard. Mater. 153 (2008) 1275–1287.

[24] A. Stafiej, K. Pyrzynska, Adsorption of heavy metal ions with carbon nanotubes, Sep. Purif. Technol. 58 (2007) 49–52.

[25] R.K. Tiwari, S.K. Ghosh, D.C. Rupainwar, Y.C. Sharma, Managing aqueous solutions rich in Mn(II): an inexpensive technique, Colloids Surf. A: Physicochem. Eng. Asp. 70 (1993) 131–137.

[26] Ö. Yavuz, Y. Altunkaynak, F. Güzel, Removal of copper, nickel, cobalt and manganese from aqueous solution by kaolinite, Water Res. 37 (2003) 948–952.

[27] A. Üçer, A. Uyanik, Ş.F. Aygün, Adsorption of Cu(II), Cd(II), Zn(II), Mn(II) and Fe(III) ions by tannic acid immobilised activated carbon, Sep. Purif. Technol. 47 (2006) 113–118.

[28] J.W. Shim, S.J. Park, S.K. Ryu, Effect of modification with HNO_3 and NaOH on metal adsorption by pitch-based activated carbon fibers, Carbon 39 (2001) 1635–1642.